

# IME: Integrating Multi-curvature Shared and Specific Embedding for Temporal Knowledge Graph Completion

Jiapu Wang\*  
Beijing University of Technology  
Beijing, China  
jpwang@emails.bjut.edu.cn

Zheng Cui\*  
Beijing University of Technology  
Beijing, China  
CuiZ@emails.bjut.edu.cn

Boyue Wang†  
Beijing University of Technology  
Beijing, China  
wby@bjut.edu.cn

Shirui Pan  
Griffith University  
Gold Coast, Australia  
s.pan@griffith.edu.au

Junbin Gao  
The University of Sydney  
Sydney, Australia  
junbin.gao@sydney.edu.au

Baocai Yin  
Beijing University of Technology  
Beijing, China  
ybc@bjut.edu.cn

Wen Gao  
Peking University  
Beijing, China  
wgao@pku.edu.cn

## ABSTRACT

Temporal Knowledge Graphs (TKGs) incorporate a temporal dimension, allowing for a precise capture of the evolution of knowledge and reflecting the dynamic nature of the real world. Typically, TKGs contain complex geometric structures, with various geometric structures interwoven. However, existing Temporal Knowledge Graph Completion (TKGC) methods either model TKGs in a single space or neglect the heterogeneity of different curvature spaces, thus constraining their capacity to capture these intricate geometric structures. In this paper, we propose a novel Integrating Multi-curvature shared and specific Embedding (IME) model for TKGC tasks. Concretely, IME models TKGs into multi-curvature spaces, including hyperspherical, hyperbolic, and Euclidean spaces. Subsequently, IME incorporates two key properties, namely *space-shared property* and *space-specific property*. The space-shared property facilitates the learning of commonalities across different curvature spaces and alleviates the spatial gap caused by the heterogeneous nature of multi-curvature spaces, while the space-specific property captures characteristic features. Meanwhile, IME proposes an Adjustable Multi-curvature Pooling (AMP) approach to effectively retain important information. Furthermore, IME innovatively designs similarity, difference, and structure loss functions to attain the stated objective. Experimental results clearly demonstrate the superior performance of IME over existing state-of-the-art TKGC models.

\*Both authors contributed equally to this research.

†Corresponding author.

Permission to make digital or hard copies of all or part of this work for personal or classroom use is granted without fee provided that copies are not made or distributed for profit or commercial advantage and that copies bear this notice and the full citation on the first page. Copyrights for components of this work owned by others than the author(s) must be honored. Abstracting with credit is permitted. To copy otherwise, or republish, to post on servers or to redistribute to lists, requires prior specific permission and/or a fee. Request permissions from [permissions@acm.org](mailto:permissions@acm.org).  
WWW '24, May 13–17, 2024, Singapore, Singapore.

© 2024 Copyright held by the owner/author(s). Publication rights licensed to ACM.  
ACM ISBN 979-8-4007-0171-9/24/05...\$15.00  
<https://doi.org/10.1145/3589334.3645361>

## CCS CONCEPTS

• **Computing methodologies** → **Reasoning about belief and knowledge.**

## KEYWORDS

Temporal Knowledge Graph, Knowledge Graph Completion, Multi-curvature Embeddings, Adjustable Pooling

## ACM Reference Format:

Jiapu Wang, Zheng Cui, Boyue Wang, Shirui Pan, Junbin Gao, Baocai Yin, and Wen Gao. 2024. IME: Integrating Multi-curvature Shared and Specific Embedding for Temporal Knowledge Graph Completion. In *Proceedings of the ACM Web Conference 2024 (WWW '24)*, May 13–17, 2024, Singapore, Singapore. ACM, New York, NY, USA, 10 pages. <https://doi.org/10.1145/3589334.3645361>

## 1 INTRODUCTION

Knowledge Graphs (KGs) are structured collections of entities and relations, providing a semantic representation of knowledge. They serve as a powerful tool for organizing and representing real-world information in a way that machines can comprehend. Typically, knowledge in KGs is represented as *triplets*, where each node is represented as an entity, and the directed edge between nodes is denoted as a relation. For example, given one *triplet* (*Albert Einstein*, *born\_in*, *Germany*), *Albert Einstein* and *Germany* are the head and tail entities, and *born\_in* means the relation between the head and tail entities. KGs find applications in a wide array of domains, including recommendation systems [19], information retrieval [8], and semantic search [14]. They enable machines to reason about entities and their relations, uncover patterns, and make informed decisions based on the structured knowledge they encapsulate.

Acknowledging the ever-changing nature of information, Temporal Knowledge Graphs (TKGs) have arisen as a natural extension of traditional KGs. In contrast to their static counterparts, TKGs introduce the temporal dimension, enabling us to track the evolution of knowledge over time. Specifically, TKGs aim to incorporate temporal attributes with triplets for *quadruplets*: (*Albert Einstein*,

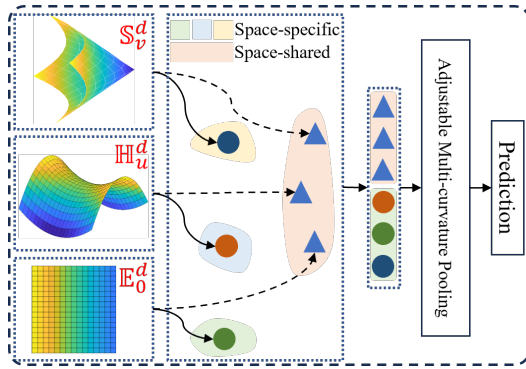


**Figure 1: A brief description of IME. Learning multi-curvature representations through *space-shared* and *space-specific* properties. These features are later utilized for subsequent predictions by the adjustable multi-curvature pooling.**

born\_in, Germany, 1879-03-14), with 1879-03-14 serving as the timestamp. Therefore, the temporal dimension allows for a systematic depiction of the trends and changes in events, thereby facilitating more context-aware and precise knowledge representation.

Despite the presence of TKGs like ICEWS [4] and GDELT [22], which encompass millions or even billions of quadruplets, the ongoing evolution of knowledge driven by natural events leaves these TKGs far from being comprehensive. The incompleteness of TKGs poses a substantial hindrance to the efficiency of knowledge-driven systems, underscoring the critical significance of "Temporal Knowledge Graph Completion (TKGC)" as an essential undertaking. The goal of the TKGC task is to enhance the completeness and accuracy of TKGs by predicting missing relations, entities, or temporal attributes that change over time within the TKGs.

The quality of the embedding representations in TKGs depends on how well the geometric structure of the embedding space matches the structure of the data. As depicted in [5, 42], various curvature spaces yield diverse impacts when embed different types of structured data. Specifically, hyperspherical space [24, 43] excels in capturing ring structures, hyperbolic space [26, 29] is highly effective in representing hierarchical arrangements, and Euclidean space proves invaluable for describing chain-like structures. However, in reality, TKGs may exhibit complex and diverse structures, resembling tree shapes in some regions and forming ring structures in others. Nonetheless, the majority of TKGC methods typically model TKGs within a singular space, posing a challenge in effectively capturing the intricate geometric structures inherent in TKGs.

The challenge of how to effectively integrate information from different curvature spaces subsequently needs to be addressed. Current TKGC methods [16, 51] typically overlook the spatial gap among different curvature spaces. Despite significant advancements, the spatial gap remains a substantial constraint on expressive capacities.

The last challenge is the feature fusion issue. Existing methods [39, 48] predominantly focus on developing sophisticated fusion mechanisms, causing a high computational complexity. Despite the effectiveness of pooling approaches like average pooling and

max pooling in reducing computational complexity, their utilization of fixed pooling strategies presents a challenge in preserving important information.

This paper proposes a novel Integrating Multi-curvature shared and specific Embedding (IME) model to address the above challenges. As shown in Figure 1, IME simultaneously models TKGs in hyperspherical, hyperbolic, and Euclidean spaces, introducing the quadruplet distributor [39] within each space to facilitate the aggregation and distribution of information among entities, relations, and timestamps. In addition, IME acquires two distinct properties for each space, encompassing both *space-shared* and *space-specific* properties. The space-shared property aids in mitigating the space gap by capturing shared information among entities, relations, and timestamps across various curvature spaces. Conversely, the space-specific property excels at fully capturing the complementary information exclusive to each curvature space. Finally, an Adjustable Multi-curvature Pooling (AMP) approach is proposed, which can learn appropriate pooling weights to get a superior pooling strategy, ultimately improving the effective retention of important information. We utilize AMP to aggregate space-shared and -specific representations of entities, relations, and timestamps to get a joint vector for downstream predictions.

The main contributions of this paper are summarized as follows:

- This paper designs a novel Multi-curvature Space-Shared and -Specific Embedding (IME) model for TKGC tasks, which learns two key properties, namely *space-shared* property and *space-specific* property. Specifically, space-shared property learns the commonalities across distinct curvature spaces and mitigates spatial gaps among them, while space-specific property captures characteristic features;
- This paper proposes an adjustable multi-curvature pooling module, designed to attain a superior pooling strategy through training for the effective retention of important information;
- To the best of our knowledge, we are the first to introduce the concept of structure loss into TKGC tasks, ensuring the structural similarity of quadruplets across various curvature spaces;
- Experimental results on several widely used datasets demonstrate that IME achieves competitive performance compared to state-of-the-art TKGC methods.

## 2 RELATED WORK

In this section, we provide an overview of KGC methods from two perspectives [27, 41]: *Euclidean embedding-based methods* and *Non-Euclidean embedding-based methods*.

### 2.1 Euclidean Embedding-based Methods

Euclidean embedding-based KGC methods typically model the KGs in the Euclidean space. Depending on the types of knowledge, we can categorize them into *static knowledge graph completion* for triplets and *temporal knowledge graph completion* for quadruplets.

**Static knowledge graph completion (SKGC)** focuses on SKGs where the information about entities and relations remains unchanged over time. The task of SKGC methods aims to predict missing triplets (e.g., relations between entities) based on known

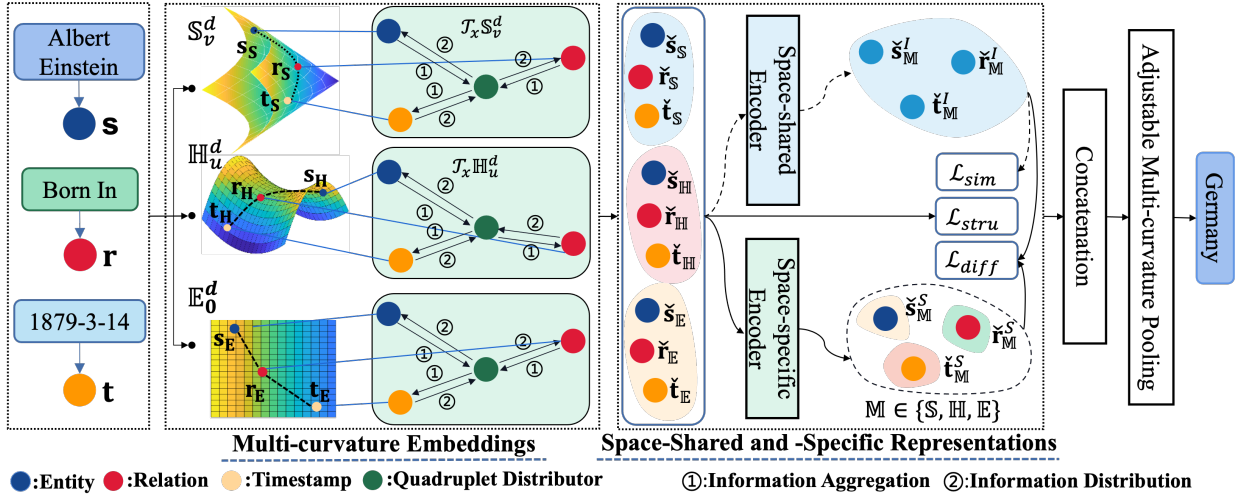


**Figure 2: The framework of IME.** Specifically, IME models the query (*Albert Einstein, Born In, ?, 1879-3-14*) in multi-curvature spaces through information aggregation and information distribution. Subsequently, IME explores *space-shared* and *space-specific* properties to learn the commonalities and characteristics across different curvature spaces, effectively reducing spatial gaps among them. Finally, these identified features are employed for adjustable multi-curvature pooling in subsequent predictions.

information. Several popular SKGC methods include McRL [38], TDN [40], and ConvE [10].

*Translation-based methods* take the relation as a translation from the head entity to the tail entity, such as TransE [3] and RotatE [33]. RotatE regards the relation as a rotation from the head entity to the tail entity in the complex space. Based on TransE, TransR [23] learns a unified mapping matrix to model the entities and relations into a common space. Simple [18] improves upon the complex Canonical Polyadic (CP) decomposition [17] by enabling the interdependent learning of the two embeddings for each entity within the complex space. Furthermore, BoxE [1] introduces the box embedding method as a means to model the uncertainty and diversity inherent in knowledge.

*Semantic matching-based methods* employ a similarity-based scoring function to evaluate the probabilities of triplets, such as DistMult [47] and McRL [38]. DistMult employs matrix multiplication to model the interaction between the entity and relation. ComplEx [34] operates within the complex space to calculate the score of the triplet. CapsE [36] introduces the capsule network to capture the hierarchical relations and semantic information among entities. TuckER [2] explores Tucker decomposition into the SKGC task. In addition, McRL [38] captures the complex conceptual information hidden in triplets to acquire accurate representations of entities and relations. MLI [37] simultaneously captures the coarse-grained and fine-grained information to enhance the information interaction.

*Convolutional neural network-based methods* explore the use of CNN to capture the inherent correlations within triplets. ConvE [10] first employs the CNN into the SKGC task. R-GCN [30] explores the graph neural network to update entity embeddings. Moreover, TDN [40] creatively designs the triplet distributor to facilitate the information transmission between entities and relations.

**Temporal knowledge graph completion (TKGC)** refers to the prediction of unknown quadruplets in TKGs based on known information, including entities, relations, and timestamps. Some classic TKGCs contain ChronoR [28], TeLM [44] and BoxTE [25].

TTransE [21] models the pair of the relation and timestamp as the translation between the head entity and the tail entity. TA-TransE and TA-DistMult [12] integrate timestamps into entities using recurrent neural networks to capture the dynamic evolution of entities. Building upon RotatE, ChronoR represents relation-timestamp pairs as rotations from the head entity to the tail entity. Similarly, TuckERTNT [32] extends the 3rd-order tensor to the 4th-order to model quadruplets. More recently, BoxTE [25] has been introduced to enable more versatile and flexible knowledge representation.

HyTE [9] first explores the dynamic evolution of entities and relations by modeling entities and relations into the timestamp space. TeRo [46] models the temporal evolution of entities as a rotation in complex vector space, and handles time interval facts using dual complex embeddings for relations. TComplEx [20] is based on ComplEx, which expands the 3rd-order tensor into a 4th-order tensor to perform TKGC. DE-Simple [13] designs the diachronic entity embedding function to capture the dynamic evolution of entities over time, subsequently employing Simple for predicting missing items. ATiSE [45] decomposes timestamps into the trend, seasonal, and irregular components to capture the evolution of entities and relations over time. TeLM [44] employs multivector embeddings and a linear temporal regularizer to obtain entity and timestamp embeddings, respectively. EvoExplore [50] incorporates two critical factors for comprehending the evolution of TKGs: local structure describes the formation process of the graph structure in detail, and global structure reflects the dynamic topology of TKGs.

BDME [48] leverages the interaction among entities, relations, and timestamps for coarse-grained embeddings and block decomposition for fine-grained embeddings. Particularly, QDN [39] extends the triplet distributor [40] into a quadruplet distributor and designs the 4th-order tensor decomposition to facilitate the information interaction among entities, relations, and timestamps.

## 2.2 Non-Euclidean Embedding-based Methods

Non-Euclidean embedding-based methods typically embed KGs into non-Euclidean space, effectively capturing the complex geometric structure inherent to them. Some classic non-Euclidean embedding methods include ATTH [6], MuRMP [42], and BiQCap [51].

For **SKGC**, ATTH models the KG within the hyperbolic space to capture both hierarchical and logical patterns. BiQUE [15] utilizes biquaternions to incorporate multiple geometric transformations, including Euclidean rotation, which is valuable for modeling patterns like symmetry, and hyperbolic rotation, which proves effective in capturing hierarchical relations. MuRMP and GIE [5] simultaneously model the KG within multi-curvature spaces to capture the complex structure.

For **TKGC**, DyERNIE [16] embeds TKGs into multi-curvature spaces to explore the dynamic evolution guided by velocity vectors defined in the tangent space. BiQCap [51] simultaneously models each relation in Euclidean and hyperbolic spaces to represent hierarchical semantics and other relation patterns of TKGs.

## 3 PROBLEM DEFINITION

Temporal knowledge graph  $\mathcal{G} = \{\mathcal{E}, \mathcal{R}, \mathcal{T}, \mathcal{Q}\}$  is a collection of entity set  $\mathcal{E}$ , relation set  $\mathcal{R}$  and timestamp set  $\mathcal{T}$ . Specifically, each quadruplet in  $\mathcal{G}$  is denoted as  $(s, r, o, t) \in \mathcal{Q}$ , where  $s, o \in \mathcal{E}$  represent the head and tail entities,  $r \in \mathcal{R}$  denotes the relation and  $t \in \mathcal{T}$  is the timestamp. The primary objective of the TKGC task is to predict the missing tail entity when given a query  $(s, r, ?, t)$ , or the missing head entity when provided with a query  $(?, r, o, t)$ .

## 4 METHODOLOGY

In this section, we present a detailed description of IME, which can be segmented into three main stages: Multi-curvature Embeddings, Space-shared and -specific Representations, and Adjustable Multi-curvature Pooling. The whole framework of IME is illustrated in Figure 2.

### 4.1 Multi-curvature Embeddings

TKGs typically encompass intricate geometric structures, including ring, hierarchical, and chain structures. Specifically, distinct geometric structures are characterized by differing modeling capacities across various geometric spaces. We simultaneously model TKGs in multi-curvature spaces to capture the complex structures.

Inspired by QDN [39], for each curvature space, we introduce the quadruplet distributor to facilitate the information aggregation and distribution among them. This is due to the fact that entities, relations, and timestamps within each curvature space typically exist in distinct semantic spaces, hindering the information transmission among them.

Given the entity, relation, timestamp, and the initial zero-tensor of the quadruplet distributor, denoted as  $s, r, t$ , and  $q$ , we operate the *information aggregation* and *information distribution*.

**Information Aggregation** dynamically aggregates the information of entities, relations, and timestamps into the quadruplet distributor through gating functions,

$$\begin{aligned} s_{q1} &= (s - q) \odot [\sigma(s - q)] \\ r_{q1} &= (r - q) \odot [\sigma(r - q)] \\ t_{q1} &= (t - q) \odot [\sigma(t - q)], \end{aligned} \quad (1)$$

where  $\sigma$  represents the sigmoid activation function;  $\odot$  is the element-wise multiplication.

Subsequently, we employ the residual network to aggregate the information of the entity, relation, and timestamp into the quadruplet distributor,

$$\check{q} = q \oplus s_{q1} \oplus r_{q1} \oplus t_{q1}, \quad (2)$$

where  $\oplus$  is the element-wise sum.

**Information Distribution** distributes the above aggregated quadruplet distributor  $\check{q}$  to the entity  $s$ , relation  $r$  and timestamp  $t$  through gating functions,

$$\begin{aligned} s_{q2} &= (s - \check{q}) \odot [\sigma(s - \check{q})] \\ r_{q2} &= (r - \check{q}) \odot [\sigma(r - \check{q})] \\ t_{q2} &= (t - \check{q}) \odot [\sigma(t - \check{q})]. \end{aligned} \quad (3)$$

Finally, we distribute the information of quadruplet distributor into the entities, relations, and timestamps,

$$\begin{aligned} \check{s} &= s \oplus s_{q2} \\ \check{r} &= r \oplus r_{q2} \\ \check{t} &= t \oplus t_{q2}. \end{aligned} \quad (4)$$

Through the above information aggregation and information distribution process, we can obtain updated representations of entities, relations, and timestamps  $\check{s}$ ,  $\check{r}$  and  $\check{t}$ .

Similarly, we operate the above information aggregation and information distribution in multi-curvature spaces, including Euclidean, hyperbolic, and hyperspherical spaces. For each entity  $s$ , relation  $r$ , and timestamp  $t$ , we can obtain their features in three curvature spaces, namely  $\check{s}_{\mathbb{M}}$ ,  $\check{r}_{\mathbb{M}}$ , and  $\check{t}_{\mathbb{M}}$  ( $\mathbb{M} \in \{\mathbb{S}, \mathbb{H}, \mathbb{E}\}$ ). Thus, we obtain nine features.

### 4.2 Space-Shared and -Specific Representations

In order to facilitate the learning of commonalities across different curvature spaces, and comprehensively capture the characteristic features unique to each curvature space, we employ encoding functions to capture both *space-shared* and *space-specific* properties. Given the updated representations  $\check{h}_{\mathbb{M}}$  ( $h \in \{s, r, t\}$ ,  $\mathbb{M} \in \{\mathbb{S}, \mathbb{H}, \mathbb{E}\}$ ) of the entity, relation, and timestamp for different curvature spaces, we explore the gate attention mechanism to achieve the encoding functions.

**Space-shared** property focuses on recognizing commonalities across various curvature spaces to reduce spatial gaps among them. Specifically, it shares the parameters  $\mathbf{W}_I$  in encoding function  $E_I(\cdot)$  to obtain the space-shared representations. The encoding process can be denoted as,

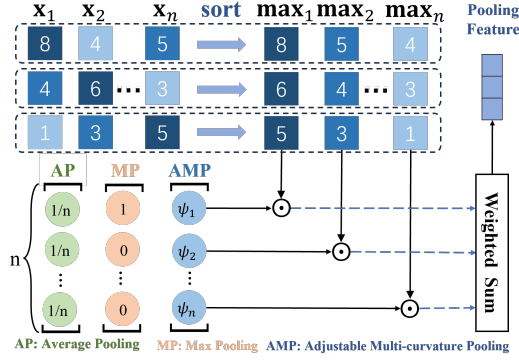


Figure 3: Comparison of different pooling approaches.

$$\begin{aligned} E_I(\check{\mathbf{h}}_S) &= \check{\mathbf{h}}_S \odot \sigma(\mathbf{W}_I^T [\check{\mathbf{h}}_S, \check{\mathbf{h}}_H, \check{\mathbf{h}}_E]) \\ E_I(\check{\mathbf{h}}_H) &= \check{\mathbf{h}}_H \odot \sigma(\mathbf{W}_I^T [\check{\mathbf{h}}_S, \check{\mathbf{h}}_H, \check{\mathbf{h}}_E]) \\ E_I(\check{\mathbf{h}}_E) &= \check{\mathbf{h}}_E \odot \sigma(\mathbf{W}_I^T [\check{\mathbf{h}}_S, \check{\mathbf{h}}_H, \check{\mathbf{h}}_E]), \end{aligned} \quad (5)$$

where  $\mathbf{W}_I$  is the shared parameter across all three curvature spaces,  $[\cdot, \cdot, \cdot]$  represents the feature concatenation operation,  $\odot$  is the element-wise multiplication,  $\sigma$  denotes the Sigmoid function. Thus, we can generate nine space-shared representations  $\mathbf{h}_M^I$  ( $\mathbf{h} \in \{s, r, t\}$ ,  $M \in \{S, H, E\}$ ) through the encoding functions  $E_I(\mathbf{h}_M)$ .

**Space-specific** property comprehensively captures the characteristic features unique to each curvature space. Similarly, it employs the encoding function  $E_S(\cdot)$  to obtain the space-specific representations,

$$\begin{aligned} E_S(\check{\mathbf{h}}_S) &= \check{\mathbf{h}}_S \odot \sigma(\mathbf{W}_{S1}^T [\check{\mathbf{h}}_S, \check{\mathbf{h}}_H, \check{\mathbf{h}}_E]) \\ E_S(\check{\mathbf{h}}_H) &= \check{\mathbf{h}}_H \odot \sigma(\mathbf{W}_{S2}^T [\check{\mathbf{h}}_S, \check{\mathbf{h}}_H, \check{\mathbf{h}}_E]) \\ E_S(\check{\mathbf{h}}_E) &= \check{\mathbf{h}}_E \odot \sigma(\mathbf{W}_{S3}^T [\check{\mathbf{h}}_S, \check{\mathbf{h}}_H, \check{\mathbf{h}}_E]), \end{aligned} \quad (6)$$

where  $\mathbf{W}_{S1}$ ,  $\mathbf{W}_{S2}$  and  $\mathbf{W}_{S3}$  are the specific parameters unique to each curvature space. Similar to the space-shared property, we can generate nine space-specific representations  $\mathbf{h}_M^S$  ( $\mathbf{h} \in \{s, r, t\}$ ,  $M \in \{S, H, E\}$ ) through the encoding functions  $E_S(\mathbf{h}_M)$ .

Through the above encoding functions  $E_I(\cdot)$  and  $E_S(\cdot)$ , we can generate eighteen space-shared and -specific vectors  $\mathbf{h}_{S/H/E}^{I/S}$  ( $\mathbf{h} \in \{s, r, t\}$ ).

### 4.3 Adjustable Multi-curvature Pooling

After obtaining the space-shared and -specific representations of entities, relations, and timestamps, the pooling approach is employed to aggregate them into a joint vector for downstream predictions. We first introduce two simple pooling approaches: Average Pooling (AP) and Max Pooling (MP). Then we introduce the proposed Adjustable Multi-curvature Pooling (AMP) approach.

As shown in Figure 3, for  $n$  input features  $\mathbf{X} = \{x_1, x_2, \dots, x_n\}$ ,  $x_i \in \mathcal{R}^{d_x}$ , we first sort each dimension of  $n$  features to extract the significant information, obtaining the sorted features  $\mathbf{M} = \{\max_1, \max_2, \dots, \max_n\}$ ,  $\max_i \in \mathcal{R}^{d_x}$ . Then we introduce the

pooling weights  $\Psi = \{\psi_1, \psi_2, \dots, \psi_n\}$ ,  $\psi_i \in \mathcal{R}^1$ , which are used to perform a weighted sum over  $\mathbf{M}$  to get pooling feature  $\mathbf{x}_p \in \mathcal{R}^{d_x}$ ,

$$\mathbf{x}_p = \sum_{i=1}^n \psi_i \cdot \max_i. \quad (7)$$

**Average Pooling** sets all pooling weights  $\psi_i$  to  $\frac{1}{n}$  to get pooling feature  $\mathbf{x}_{ap} \in \mathcal{R}^{d_x}$ ,

$$\mathbf{x}_{ap} = \sum_{i=1}^n \frac{1}{n} \cdot \max_i. \quad (8)$$

**Max Pooling** sets the first pooling weight  $\psi_1$  to 1 and the others  $\psi_i, i \neq 1$  to 0 to get pooling feature  $\mathbf{x}_{mp} \in \mathcal{R}^{d_x}$ ,

$$\mathbf{x}_{mp} = \max_1. \quad (9)$$

However, the aforementioned two pooling approaches rely on fixed pooling strategies, posing a challenge in ensuring the effective retention of important information.

**Adjustable Multi-curvature Pooling** automatically adjusts pooling weights to obtain a superior pooling strategy, effectively retaining important information. To learn appropriate pooling weights  $\Psi$  for the different positions of  $\mathbf{M}$ , i.e.  $\max_i$ , we first utilize the positional encoding strategy in [7, 35] to get positional encoding  $\mathbf{P} = \{\mathbf{p}_1, \mathbf{p}_2, \dots, \mathbf{p}_n\}$ ,  $\mathbf{p}_i \in \mathcal{R}^{d_p}$ . This positional encoding  $\mathbf{P}$  contains prior information between position indices, and can be formulated as follows,

$$\begin{aligned} \mathbf{p}_i(2k) &= \sin\left(\frac{i}{10000^{2k/d_p}}\right) \\ \mathbf{p}_i(2k+1) &= \cos\left(\frac{i}{10000^{2k/d_p}}\right), \end{aligned} \quad (10)$$

where  $k$  indicates the dimension. Then we regard the sequence of positional encoding  $\mathbf{P}$  as input and utilize Bi-GRU [31] and Multi-Layer Perceptron (MLP) to obtain pooling weights  $\Psi$ ,

$$\Psi = \text{MLP}(\text{Bi-GRU}(\mathbf{P})). \quad (11)$$

Further,  $\Psi$  is normalized as follows,

$$\psi_i = \frac{\exp(\psi_i)}{\sum_{j=1}^n \exp(\psi_j)}. \quad (12)$$

Based on the learned pooling weights, we get the pooling feature  $\mathbf{x}_{amp} \in \mathcal{R}^{d_x}$ ,

$$\mathbf{x}_{amp} = \sum_{i=1}^n \psi_i \cdot \max_i. \quad (13)$$

According to (10), (11), (12) and (13), the entire calculation process of AMP can be integrated as follows,

$$\mathbf{x}_{amp} = \text{AMP}(\mathbf{X}, \theta), \quad (14)$$

where  $\theta$  indicates all the learnable parameters.

**Pooling Procedure.** We concatenate the space-shared and space-specific representations of the entity, relation and timestamp into  $\mathbf{H} = \{\mathbf{h}_S^I, \mathbf{h}_H^I, \mathbf{h}_E^I, \mathbf{h}_S^S, \mathbf{h}_H^S, \mathbf{h}_E^S\}$  ( $\mathbf{h} \in \{s, r, t\}$ ). Subsequently, we employ the AMP approach to effectively retain important information

**Table 1: Statistic information of whole datasets.**

Datasets	#Entities	#Relations	#Timestamps	#Time Span	#Granularity	#Training	#Validation	#Test
ICEWS14	6,869	230	365	2014	1 day	72,826	8,941	8,963
ICEWS05-15	10,094	251	4,017	2005-2015	1 day	368,962	46,275	46,092
GDELT	500	20	366	2015-2016	1 day	2,735,685	341,961	341,961

among entities, relations, and timestamps, and the score function can be defined as follows,

$$f(\mathbf{s}, \mathbf{r}, \mathbf{o}, \mathbf{t}) = \langle \text{AMP}(\mathbf{H}, \theta), \mathbf{o} \rangle, \quad (15)$$

where  $\langle \cdot, \cdot \rangle$  represents the inner product operation.

#### 4.4 Loss Function

In this section, we propose the overall loss of the proposed model IME as follows,

$$\mathcal{L} = \mathcal{L}_{task} + \alpha \mathcal{L}_{sim} + \beta \mathcal{L}_{diff} + \gamma \mathcal{L}_{stru}, \quad (16)$$

where  $\alpha, \beta, \gamma$  are the hyper-parameters. Each component within the loss is responsible for achieving the desired properties.

**Task Loss.** Following the strategy in [44], we explore the cross-entropy and standard data augmentation protocol to achieve the multi-class task,

$$\begin{aligned} \mathcal{L}_{task} = & -\log\left(\frac{\exp(f(\mathbf{s}, \mathbf{r}, \mathbf{o}, \mathbf{t}))}{\sum_{\mathbf{s}' \in \mathcal{E}} \exp(f(\mathbf{s}', \mathbf{r}, \mathbf{o}, \mathbf{t}))}\right) \\ & -\log\left(\frac{\exp(f(\mathbf{o}, \mathbf{r}^{-1}, \mathbf{s}, \mathbf{t}))}{\sum_{\mathbf{o}' \in \mathcal{E}} \exp(f(\mathbf{o}', \mathbf{r}^{-1}, \mathbf{s}, \mathbf{t}))}\right). \end{aligned} \quad (17)$$

**Similarity Loss.** The purpose of the similarity loss is to minimize the disparities among shared features across different curvature spaces, aiming to bridge spatial gaps among them. Specifically, Central Moment Discrepancy (CMD) [49] is a distance metric employed to evaluate the similarity between two distributions by quantifying the discrepancy in their central moments. A smaller CMD value indicates a higher similarity between the two distributions. Let  $X$  and  $Y$  be bounded independent and identically distributed random vectors from two probability distributions,  $p$  and  $q$ , defined on the interval  $[a, b]$ . The CMD can be defined as,

$$\begin{aligned} \text{CMD}(X, Y) = & \frac{1}{|b-a|} \| \mathbf{E}(X) - \mathbf{E}(Y) \|_2 \\ & + \sum_{k=2}^{\infty} \frac{1}{|b-a|^k} \| c_k(X) - c_k(Y) \|_2, \end{aligned} \quad (18)$$

where  $\mathbf{E}(X)$  is the expectation of  $X$ , and  $c_k(x) = \mathbf{E}((X - \mathbf{E}(X))^k)$  is the central moment vector of order  $k$ .

In our case, we calculate the similarity loss through CMD,

$$\mathcal{L}_{sim} = \frac{1}{3} \sum_{(\mathbb{M}_1, \mathbb{M}_2)} \text{CMD}(\mathbf{h}_{\mathbb{M}_1}^S, \mathbf{h}_{\mathbb{M}_2}^S) \quad (19)$$

where  $(\mathbb{M}_1, \mathbb{M}_2) \in \{(\mathbb{E}, \mathbb{H}), (\mathbb{E}, \mathbb{S}), (\mathbb{H}, \mathbb{S})\}$ .

**Difference Loss.** The difference loss is designed to capture characteristic features of different curvature spaces through a similarity function. Specifically, we not only impose the soft orthogonality constraint between the shared and specific features but also between the space-specific features. The difference loss is calculated as:

$$\mathcal{L}_{diff} = \sum_{\mathbb{M}} \| (\mathbf{h}_{\mathbb{M}}^S)^T \mathbf{h}_{\mathbb{M}}^I \|_F^2 + \sum_{(\mathbb{M}_1, \mathbb{M}_2)} \| (\mathbf{h}_{\mathbb{M}_1}^S)^T \mathbf{h}_{\mathbb{M}_2}^S \|_F^2, \quad (20)$$

where  $\mathbb{M} \in \{\mathbb{S}, \mathbb{H}, \mathbb{E}\}$ ,  $(\mathbb{M}_1, \mathbb{M}_2) \in \{(\mathbb{E}, \mathbb{H}), (\mathbb{E}, \mathbb{S}), (\mathbb{H}, \mathbb{S})\}$ ,  $\| \cdot \|_F^2$  is the squared Frobenius norm.

**Structure Loss.** The structure loss [11] aims to ensure the structural similarity of quadruplets across various curvature spaces. Specifically, we define the relation on a triplet of samples  $(\mathbf{x}_a, \mathbf{x}_b, \mathbf{x}_c)$  as the following cosine value:

$$\cos \angle \mathbf{r}_a \mathbf{r}_b \mathbf{r}_c = \langle \mathbf{e}^{ab}, \mathbf{e}^{cb} \rangle \quad \text{where} \quad \mathbf{e}^{ij} = \frac{\mathbf{r}_i - \mathbf{r}_j}{\| \mathbf{r}_i - \mathbf{r}_j \|_2} \quad (21)$$

where  $\mathbf{r}_*$  is sample. Thus, the structure loss can be calculated as,

$$\mathcal{L}_{stru} = \frac{1}{3} \sum_{(\mathbb{M}_1, \mathbb{M}_2)} \| \cos \angle \mathbb{M}_{1a} \mathbb{M}_{1b} \mathbb{M}_{1c} - \cos \angle \mathbb{M}_{2a} \mathbb{M}_{2b} \mathbb{M}_{2c} \|_1, \quad (22)$$

where  $(\mathbb{M}_1, \mathbb{M}_2) \in \{(\mathbb{E}, \mathbb{H}), (\mathbb{E}, \mathbb{S}), (\mathbb{H}, \mathbb{S})\}$ .

## 5 EXPERIMENT

In this section, we provide detailed information about the datasets, describe the experimental setups, present experimental results, and conduct a comprehensive analysis of experimental results.

### 5.1 Datasets

We provide a list of three commonly-used TKG datasets and their key statistics are summarized in Table 1. **ICEWS14** and **ICEWS05-15** [12] are subsets of *Integrated Crisis Early Warning System (ICEWS)*, which encompass various political events along with their respective timestamps. **GDELT** [22] is a subset of the larger *Global Database of Events, Language, and Tone (GDELT)* that includes data on human social relationships.

### 5.2 Baselines

The proposed model is compared with some classic KGC methods, including SKGC and TKGC methods.

- **SKGC methods:** TransE [3], DistMult [47], Simple [18], RotatE [33];
- **TKGC methods:** TA-DistMult [12], TeRo [46], ChronoR [28], ATiSE [45], TeLM [44], TuckERTNT [32], BoxTE [25], BDME [48], EvoExplore [50], DyERNIE [16], BiQCap [51], and QDN [39].

### 5.3 Link Prediction Metrics

We substitute either the head or tail entity in each test quadruplet  $(\mathbf{s}, \mathbf{r}, \mathbf{o}, \mathbf{t})$  with all feasible entities sampled from the TKG. Subsequently, we rank the scores calculated by the score function. We employ Mean Reciprocal Rank (MRR) and Hit@N as evaluation

**Table 2: Link prediction results on ICEWS14, ICEWS05-15, and GDELT datasets. The best results are in bold and the second results are underlined. - means the result is unavailable.**

Datasets	ICEWS14				ICEWS05-15				GDELT			
	MRR	Hit@1	Hit@3	Hit@10	MRR	Hit@1	Hit@3	Hit@10	MRR	Hit@1	Hit@3	Hit@10
TransE (2013)	0.280	0.094	–	0.637	0.294	0.090	–	0.663	0.113	0.0	0.158	0.312
DistMult (2015)	0.439	0.323	–	0.672	0.456	0.337	–	0.691	0.196	0.117	0.208	0.348
Simple (2018)	0.458	0.341	0.516	0.687	0.478	0.359	0.539	0.708	0.206	0.124	0.220	0.366
RotatE (2019)	0.418	0.291	0.478	0.690	0.304	0.164	0.355	0.595	–	–	–	–
TA-DistMult (2018)	0.477	0.363	–	0.686	0.474	0.346	–	0.728	0.206	0.124	0.219	0.365
ATiSE (2019)	0.550	0.436	0.629	0.750	0.519	0.378	0.606	0.794	–	–	–	–
TeRo (2020)	0.562	0.468	0.621	0.732	0.586	0.469	0.668	0.795	0.245	0.154	0.264	0.420
ChronoR (2021)	0.625	0.547	0.669	0.773	0.675	0.596	0.723	0.820	–	–	–	–
TeLM (2021)	0.625	0.545	0.673	0.774	0.678	0.599	0.728	0.823	–	–	–	–
TuckERTNT (2022)	0.604	0.521	0.655	0.753	0.638	0.559	0.686	0.783	0.381	0.283	0.418	0.576
BoxTE (2022)	0.613	0.528	0.664	0.763	0.667	0.582	0.719	0.820	0.352	0.269	0.377	0.511
EvoExplore (2022)	<u>0.725</u>	<u>0.653</u>	<u>0.778</u>	<u>0.852</u>	<u>0.790</u>	<u>0.719</u>	<b>0.843</b>	<b>0.915</b>	0.514	0.353	<u>0.602</u>	<u>0.748</u>
BDME (2023)	0.635	0.555	0.683	0.778	–	–	–	–	0.278	0.191	0.299	0.448
QDN (2023)	0.643	0.567	0.688	0.784	0.692	0.611	0.743	0.838	<u>0.545</u>	<u>0.481</u>	0.576	0.668
DyERNIE (2020)	0.669	0.599	0.714	0.797	0.739	0.679	0.773	0.855	0.457	0.390	0.479	0.589
BiQCap (2023)	0.643	0.563	0.687	0.798	0.691	0.621	0.738	0.837	0.273	0.183	0.308	0.469
IME	<b>0.819</b>	<b>0.790</b>	<b>0.835</b>	<b>0.872</b>	<b>0.796</b>	<b>0.750</b>	<u>0.821</u>	<u>0.875</u>	<b>0.624</b>	<b>0.485</b>	<b>0.754</b>	<b>0.791</b>

metrics, with  $N=1, 3$  and  $10$ . Higher values indicate better performance. Finally, we present the *filtered* results as final experimental results, which exclude all corrupted quadruplets from the TKG.

## 5.4 Parameters Setting

We use a grid search to find the best hyper-parameters based on the MRR performance on the validation dataset. Specifically, we tune the similarity loss weight  $\alpha$ , the difference loss weight  $\beta$ , and the structure loss weight  $\gamma$ , choosing from  $\{0.1, 0.2, \dots, 0.9\}$ . The optimal  $\alpha$ ,  $\beta$  and  $\gamma$  on different datasets are set as follows:  $\alpha = 0.4$ ,  $\beta = 0.4$  and  $\gamma = 0.1$  for ICEWS14;  $\alpha = 0.9$ ,  $\beta = 0.3$  and  $\gamma = 0.1$  for ICEWS05-15;  $\alpha = 1$ ,  $\beta = 0.3$  and  $\gamma = 0.1$  for GDELT. We set the optimal embedding dimension  $D$  to 500 across all datasets. For the AMP approach, the dimension of positional encoding is set to 32, i.e.,  $d_p$  is set to 32. The dimension of Bi-GRU is also set to 32 and MLP is used to project features from 32 dimensions to 1.

Moreover, the learning rate is fine-tuned within the range  $\{0.1, 0.05, 0.01, 0.005, 0.001\}$  on different datasets, ultimately being set to 0.1 for all datasets. The batch size of 1000 is consistently applied across all datasets. The entire experiment is implemented using the PyTorch 1.8.1 platform and conducted on a single NVIDIA RTX A6000 GPU.

## 5.5 Experimental Results and Analysis

The link prediction experimental results are displayed in Table 2, and the experimental analyses are listed as follows:

(1) The proposed model outperforms state-of-the-art baselines on three datasets, showing clear superiority in most metrics. For example, the proposed model obtains 9.4% and 0.6% improvements over EvoExplore under MRR on ICEWS14 and ICEWS05-15, respectively. This phenomenon indicates that a single space is insufficient for modeling complex geometric structures concurrently, and the

spatial gap in multi-curvature spaces severely limits the expressive capacity of TKGC models.

(2) BiQCap [51] and DyERNIE [16] are two important baselines because they both model TKGs in multi-curvature spaces. However, our proposed method still improves most metrics for all datasets. This phenomenon reflects that our proposed method can effectively reduce spatial gaps caused by the heterogeneity of different curvature spaces.

(3) QDN [39] is also an essential baseline because it serves as a key component of the multi-curvature embeddings module. When compared to QDN, our proposed method exhibits a substantial improvement in performance across all metrics. This observation underscores the inadequacy of a single Euclidean space for modeling complex geometric structures.

These observations indicate that our proposed method can not only model complex geometric structures but also effectively reduce spatial gaps among different curvature spaces.

## 5.6 Impact of Loss Weights $\alpha$ , $\beta$ , and $\gamma$

In this experiment, we explore the influence of changing the loss weights  $\alpha$ ,  $\beta$ , and  $\gamma$  on MRR. As depicted in Figure 4, it becomes evident that with increasing weight, various loss functions display noteworthy differences in performance. To be specific, the similarity loss  $\alpha$  and the difference loss  $\beta$  display a parabolic shape, with their peaks occurring at 0.4. In contrast, the structure loss  $\gamma$  reveals an overall declining trend, gradually diminishing as the weight increases.

These phenomena clearly illustrate that appropriate weights for similarity and difference losses effectively facilitate the learning of common and characteristic features of entities, relations, and timestamps across multiple curvature spaces. Conversely, a higher weight for the structure loss restricts their flexibility in embeddings across these multiple curvature spaces.

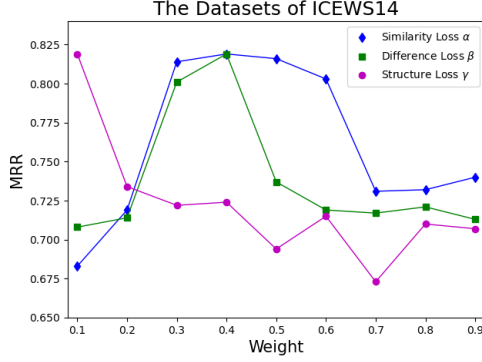


Figure 4: H@1 with varying loss weights  $\alpha$ ,  $\beta$  and  $\gamma$  on ICEWS14.

Table 3: The ablation experiment results on ICEWS14. “w/o” represents removal for the mentioned factors, “(-)” denotes replacing Adjustable Multi-curvature Pooling (AMP) with the mentioned factors. We mark the better results in bolded.

Datasets	ICEWS14			
	MRR	Hit@1	Hit@3	Hit@10
DistMult (2015)	0.439	0.323	-	0.672
TA-DistMult (2018)	0.477	0.363	-	0.686
IME (-) MP	0.523	0.430	0.574	0.696
IME w/o $\mathcal{L}_{sim}$	0.740	0.693	0.765	0.824
IME w/o $\mathcal{L}_{diff}$	0.716	0.653	0.752	0.835
IME w/o $\mathcal{L}_{stru}$	0.810	0.760	0.810	0.859
IME	<b>0.819</b>	<b>0.790</b>	<b>0.835</b>	<b>0.872</b>

<sup>1</sup> MP represents Max Pooling.

## 5.7 Ablation Experiments

In order to investigate the impact of key modules and loss functions on experimental performance, we conducted a series of ablation experiments, and the corresponding link prediction results are presented in Table 3.

- i. “IME w/o  $\mathcal{L}_{sim}$ ”, “IME w/o  $\mathcal{L}_{diff}$ ”, and “IME w/o  $\mathcal{L}_{stru}$ ” mean removing the similarity loss  $\mathcal{L}_{sim}$ , difference loss  $\mathcal{L}_{diff}$ , and structure loss  $\mathcal{L}_{stru}$ ;
- ii. “IME (-) MP” represents replacing Adjustable Multi-curvature Pooling (AMP) with the Max Pooling (MP).

(1) In the first category of ablation experiments, the proposed model achieves a significant improvement on ICEWS14. For example, compared to “IME w/o  $\mathcal{L}_{sim}$ ”, “IME w/o  $\mathcal{L}_{diff}$ ”, and “IME w/o  $\mathcal{L}_{stru}$ ”, the proposed model achieves 7.9%, 10.3%, and 0.9% improvements on Hit@1, respectively. Thus, we can summarize the following conclusions:

- a) Similarity loss can effectively learn the commonalities across distinct curvature spaces and mitigate spatial gaps among them;
- b) Difference loss can capture characteristic features specific to each space;

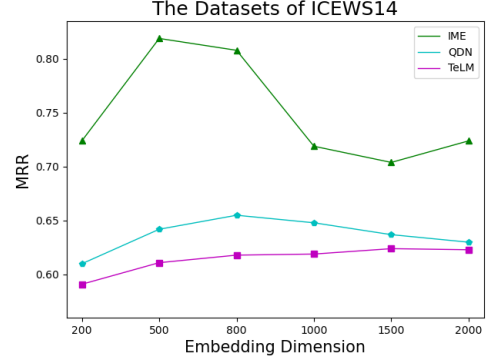


Figure 5: Comparison of MRR performance with different embedding dimensions on ICEWS14.

- c) Structure loss serves to constrain the embeddings of entities, relations, and timestamps by ensuring that information in distinct spaces exhibits comparable geometric structures.

(2) In the second category of ablation experiments, the proposed model exhibits a certain improvement on ICEWS14. This phenomenon demonstrates that the adjustable multi-curvature pooling approach can effectively strengthen the important information for modeling the current TKG while weakening the undesirable ones.

## 5.8 Impact of Embedding Dimensions $D$

To empirically investigate the impact of embedding dimensions on ICEWS14, we fine-tune the dimension  $D$  within the range of {200, 500, 800, 1000, 1500, 2000} and analyze the experimental results. As shown in Figure 5, the MRR performance on ICEWS14 exhibits an initial increase followed by a decrease as the dimension increases, eventually peaking at  $D = 500$ .

This phenomenon implies that the proposed model faces challenges in capturing intricate data relationships at lower dimensions, resulting in poorer performance. As the dimension increases, the model becomes more capable of effectively representing data, leading to enhanced performance. Nevertheless, beyond a certain threshold, this may introduce some issues such as overfitting or heightened complexity, consequently causing a decline in performance.

## 6 CONCLUSION

In this paper, we proposed a novel TKGC method called Integrating Multi-curvature shared and specific Embedding (IME). Specifically, IME models TKGs in multi-curvature spaces to capture complex geometric structures. Meanwhile, IME learns the space-specific property to comprehensively capture characteristic information, and the space-shared property to reduce spatial gaps caused by the heterogeneity of different curvature spaces. Furthermore, IME innovatively proposes an Adjustable Multi-curvature Pooling (AMP) approach to effectively strengthen the retention of important information. Experimental results on several well-established datasets incontrovertibly show that IME achieves competitive performance when compared to state-of-the-art TKGC methods.

## ACKNOWLEDGMENTS

This work was funded by the National Key R&D Program of China (No. 2021ZD0111902), National Natural Science Foundation of China (No. 92370102, 62272015, U21B2038), R&D Program of Beijing Municipal Education Commission (KZ202210005008).

## REFERENCES

- [1] Ralph Abboud, Ismail Ceylan, Thomas Lukasiewicz, and Tommaso Salvatori. 2020. BoxE: A box embedding model for knowledge base completion. In *Neural Information Processing Systems*. 9649–9661.
- [2] Ivana Balažević, Carl Allen, and Timothy M Hospedales. 2019. Tucker: Tensor factorization for knowledge graph completion. In *Empirical Methods in Natural Language Processing*. 5185–5194.
- [3] Antoine Bordes, Nicolas Usunier, Alberto Garcia-Duran, Jason Weston, and Oksana Yakhnenko. 2013. Translating embeddings for modeling multi-relational data. In *Neural Information Processing Systems*. 2787–2795.
- [4] Elizabeth Boschee, Jennifer Lautenschlager, Sean O'Brien, Steve Shellman, James Starz, and Michael Ward. 2015. ICEWS Coded Event Data. In *Harvard Dataverse*.
- [5] Zongsheng Cao, Qianqian Xu, Zhiyong Yang, Xiaochun Cao, and Qingming Huang. 2022. Geometry interaction knowledge graph embeddings. In *AAAI Conference on Artificial Intelligence*.
- [6] Ines Chami, Adva Wolf, Da Cheng Juan, Frederic Sala, Sujith Ravi, and Christopher Ré. 2020. Low-dimensional hyperbolic knowledge graph embeddings. In *Annual Meeting of the Association for Computational Linguistics*. 6901–6914.
- [7] Jiacheng Chen, Hexiang Hu, Hao Wu, Yuning Jiang, and Changhuo Wang. 2021. Learning the best pooling strategy for visual semantic embedding. In *Proceedings of the IEEE/CVF conference on computer vision and pattern recognition*. 15789–15798.
- [8] Jeffrey Dalton, Laura Dietz, and James Allan. 2014. Entity query feature expansion using knowledge base links. In *ACM SIGIR Conference on Research & Development in Information Retrieval*. 365–374.
- [9] Shib Sankar Dasgupta, Swayambhu Nath Ray, and Partha Talukdar. 2018. HyTE: Hyperplane-based temporally aware knowledge graph embedding. In *Empirical Methods in Natural Language Processing*. 2001–2011.
- [10] Tim Dettmers, Pasquale Minervini, Pontus Stenetorp, and Sebastian Riedel. 2018. Convolutional 2D knowledge graph embeddings. In *AAAI Conference on Artificial Intelligence*. 1811–1818.
- [11] Qiankun Gao, Chen Zhao, Bernard Ghanem, and Jian Zhang. 2022. R-DFCIL: Relation-guided representation learning for data-free class incremental learning. In *European Conference on Computer Vision*. 423–439.
- [12] Alberto Garcia-Durán, Sebastijan Dumančić, and Mathias Niepert. 2018. Learning sequence encoders for temporal knowledge graph completion. In *Empirical Methods in Natural Language Processing*. 4816–4821.
- [13] Rishab Goel, Seyed Mehran Kazemi, Marcus Brubaker, and Pascal Poupard. 2020. Diachronic embedding for temporal knowledge graph completion. In *AAAI Conference on Artificial Intelligence*. 3988–3995.
- [14] Ramanathan Guha, Rob McCool, and Eric Miller. 2003. Semantic search. In *Proceedings of the 12th international conference on World Wide Web*. 700–709.
- [15] Jia Guo and Stanley Kok. 2021. BiQUE: Biquaternionic Embeddings of Knowledge Graphs. In *Proceedings of the Conference on Empirical Methods in Natural Language Processing*. 8338–8351.
- [16] Zhen Han, Yunpu Ma, Peng Chen, and Volker Tresp. 2020. DyERNIE: Dynamic evolution of riemannian manifold embeddings for temporal knowledge graph completion. In *Empirical Methods in Natural Language Processing*. 7301–7316.
- [17] Frank L Hitchcock. 1927. The expression of a tensor or a polyadic as a sum of products. *Journal of Mathematics and Physics* 6, 1-4 (1927), 164–189.
- [18] Seyed Mehran Kazemi and David Poole. 2018. Simple embedding for link prediction in knowledge graphs. In *Neural Information Processing Systems*. 4284–4295.
- [19] Hyeyoung Ko, Suyeon Lee, Yoonseo Park, and Anna Choi. 2022. A survey of recommendation systems: recommendation models, techniques, and application fields. *Electronics* 11, 1 (2022), 141.
- [20] Timothée Lacroix, Guillaume Obozinski, and Nicolas Usunier. 2020. Tensor decompositions for temporal knowledge base completion. In *International Conference on Learning Representations*. 1–12.
- [21] Julien Leblay and Melisachew Wudage Chekol. 2018. Deriving validity time in knowledge graph. In *International Conference on World Wide Web*. 1771–1776.
- [22] Kalev Leetaru and Philip A Schrodt. 2013. GDELT: Global data on events, location, and tone. In *ISA Annual Convention*. 1–49.
- [23] Yankai Lin, Zhiyuan Liu, Maosong Sun, Yang Liu, and Xuan Zhu. 2015. Learning entity and relation embeddings for knowledge graph completion. In *AAAI Conference on Artificial Intelligence*. 2181–2187.
- [24] Weiyang Liu, Yandong Wen, Zhiding Yu, Ming Li, Bhiksha Raj, and Le Song. 2017. SpheroFace: Deep hypersphere embedding for face recognition. In *the Conference on Computer Vision and Pattern Recognition*. 212–220.
- [25] Johannes Messner, Ralph Abboud, and Ismail Ilkan Ceylan. 2022. Temporal knowledge graph completion using box embeddings. In *AAAI Conference on Artificial Intelligence*. 7779–7787.
- [26] Maximilian Nickel and Douwe Kiela. 2017. Poincaré embeddings for learning hierarchical representations. In *Advances in Neural Information Processing Systems*.
- [27] Shirui Pan, Linhao Luo, Yufei Wang, Chen Chen, Jiapu Wang, and Xindong Wu. 2024. Unifying Large Language Models and Knowledge Graphs: A Roadmap. *IEEE Transactions on Knowledge and Data Engineering* (2024), 1–20.
- [28] Ali Sadeghian, Mohammadreza Armandpour, Anthony Colas, and Daisy Zhe Wang. 2021. ChronoR: rotation based temporal knowledge graph embedding. In *AAAI Conference on Artificial Intelligence*. 6471–6479.
- [29] Frederic Sala, Chris De Sa, Albert Gu, and Christopher Ré. 2018. Representation tradeoffs for hyperbolic embeddings. In *International Conference on Machine Learning*. 4460–4469.
- [30] Michael Schlichtkrull, Thomas N Kipf, Peter Bloem, Rianne Van Den Berg, Ivan Titov, and Max Welling. 2018. Modeling relational data with graph convolutional networks. In *European Semantic Web Conference*. Springer, 593–607.
- [31] Mike Schuster and Kuldeep K Paliwal. 1997. Bidirectional recurrent neural networks. *IEEE transactions on Signal Processing* 45, 11 (1997), 2673–2681.
- [32] Pengpeng Shao, Dawei Zhang, Guohua Yang, Jianhua Tao, Feihu Che, and Tong Liu. 2022. Tucker decomposition-based temporal knowledge graph completion. *Knowledge-Based Systems* 238 (2022), 107841.
- [33] Zhiqing Sun, Zhi-Hong Deng, Jian-Yun Nie, and Jian Tang. 2019. RotatE: Knowledge graph embedding by relational rotation in complex space. In *International Conference on Learning Representations*. 1–18.
- [34] Théo Trouillon, Johannes Welbl, Sebastian Riedel, Éric Gaussier, and Guillaume Bouchard. 2016. Complex embeddings for simple link prediction. In *International Conference on Machine Learning*. 2071–2080.
- [35] Ashish Vaswani, Noam Shazeer, Niki Parmar, Jakob Uszkoreit, Llion Jones, Aidan N Gomez, Łukasz Kaiser, and Illia Polosukhin. 2017. Attention is all you need. *Advances in neural information processing systems* 30 (2017).
- [36] Thanh Vu, Tu Dinh Nguyen, Dat Quoc Nguyen, Dinh Phung, et al. 2019. A capsule network-based embedding model for knowledge graph completion and search personalization. In *Proceedings of the Conference of the Association for Computational Linguistics: Human Language Technologies*. 2180–2189.
- [37] Jiapu Wang, Boyue Wang, Junbin Gao, Simin Hu, Yongli Hu, and Baocai Yin. 2024. Multi-Level Interaction Based Knowledge Graph Completion. *IEEE/ACM Transactions on Audio, Speech, and Language Processing* 32 (2024), 386–396.
- [38] Jiapu Wang, Boyue Wang, Junbin Gao, Yongli Hu, and Baocai Yin. 2022. Multi-concept Representation Learning for Knowledge Graph Completion. *ACM Transactions on Knowledge Discovery from Data* (2022).
- [39] Jiapu Wang, Boyue Wang, Junbin Gao, Xiaoyan Li, Yongli Hu, and Baocai Yin. 2023. QDN: A Quadruplet Distributor Network for Temporal Knowledge Graph Completion. *IEEE Transactions on Neural Networks and Learning Systems* (2023).
- [40] Jiapu Wang, Boyue Wang, Junbin Gao, Xiaoyan Li, Yongli Hu, and Baocai Yin. 2023. TDN: Triplet Distributor Network for Knowledge Graph Completion. *IEEE Transactions on Knowledge and Data Engineering* (2023).
- [41] Jiapu Wang, Boyue Wang, Meikang Qiu, Shirui Pan, Bo Xiong, Heng Liu, Linhao Luo, Tengfei Liu, Yongli Hu, Baocai Yin, et al. 2023. A Survey on Temporal Knowledge Graph Completion: Taxonomy, Progress, and Prospects. *arXiv preprint arXiv:2308.02457* (2023).
- [42] Shen Wang, Xiaokai Wei, Cicero Nogueira Nogueira dos Santos, Zhiguo Wang, Ramesh Nallapati, Andrew Arnold, Bing Xiang, Philip S Yu, and Isabel F Cruz. 2021. Mixed-curvature multi-relational graph neural network for knowledge graph completion. In *International Conference on World Wide Web*. 1761–1771.
- [43] Richard C Wilson, Edwin R Hancock, Elżbieta Pekalska, and Robert PW Duin. 2014. Spherical and hyperbolic embeddings of data. *IEEE Transactions on Pattern Analysis and Machine Intelligence* 36, 11 (2014), 2255–2269.
- [44] Chengjin Xu, Yung-Yu Chen, Mojtaba Nayyeri, and Jens Lehmann. 2021. Temporal knowledge graph completion using a linear temporal regularizer and multivector embeddings. In *Annual Meeting of the Association for Computational Linguistics*. 2569–2578.
- [45] Chenjin Xu, Mojtaba Nayyeri, Fouad Alkhoury, Hamed Yazdi, and Jens Lehmann. 2020. Temporal knowledge graph completion based on time series gaussian embedding. In *International Semantic Web Conference*. 654–671.
- [46] Chengjin Xu, Mojtaba Nayyeri, Fouad Alkhoury, Hamed Shariat Yazdi, and Jens Lehmann. 2020. TeRo: A time-aware knowledge graph embedding via temporal rotation. In *International Conference on Computational Linguistics*. 1583–1593.
- [47] Bishan Yang, Wen Tau Yih, Xiaodong He, Jianfeng Gao, and Li Deng. 2015. Embedding entities and relations for learning and inference in knowledge bases. In *International Conference on Learning Representations*. 1–13.
- [48] Lupeng Yue, Yongjian Ren, Yan Zeng, Jilin Zhang, Kaisheng Zeng, and Jian Wan. 2023. Block Decomposition with Multi-granularity Embedding for Temporal Knowledge Graph Completion. In *International Conference on Database Systems for Advanced Applications*. 706–715.

- [49] Werner Zellinger, Thomas Grubinger, Edwin Lughofer, Thomas Natschläger, and Susanne Saminger-Platz. 2017. Central Moment Discrepancy (CMD) for Domain-Invariant Representation Learning. In *International Conference on Learning Representations*. 1–13.
- [50] Jiasheng Zhang, Shuang Liang, Yongpan Sheng, and Jie Shao. 2022. Temporal knowledge graph representation learning with local and global evolutions. *Knowledge-Based Systems* 251 (2022), 109234.
- [51] Sensen Zhang, Xun Liang, Zhiying Li, Junlan Feng, Xiangping Zheng, and Bo Wu. 2023. BiQCap: A Biquaternion and Capsule Network-Based Embedding Model for Temporal Knowledge Graph Completion. In *International Conference on Database Systems for Advanced Applications*. 673–688.